Journal of Materials Research and Technology 27 (2023) 4978–4985

Contents lists available at ScienceDirect

Journal of Materials Research and Technology

journal homepage: www.elsevier.com/locate/jmrt

Phase transformation pathways in a Ti-5.9Cu alloy modified with Fe and Al

Thomas Klein [a,*], Duyao Zhang [b], Ella Staufer [c], Torben Boll [d,e,f], Christian Schneider-Broeskamp [a], Christian Edtmaier [c], Martin Schmitz-Niederau [g], Jelena Horky [h], Dong Qiu [b], Mark Easton [b]

[a] LKR Light Metals Technologies, AIT Austrian Institute of Technology, 5282, Ranshofen, Austria
[b] Centre for Additive Manufacturing, School of Engineering, RMIT University, Melbourne, Australia
[c] Institute of Chemical Technologies and Analytics, TU Wien, 1060, Vienna, Austria
[d] Karlsruhe Nano Micro Facility (KNMFi), Karlsruhe Institute of Technology, Eggenstein-Leopoldshafen, Germany
[e] Institute for Applied Materials – Materials Science and Engineering (IAM-WK), Karlsruhe Institute of Technology, Karlsruhe, Germany
[f] Institute for Nanotechnology (INT), Karlsruhe Institute of Technology, Karlsruhe, Germany
[g] voestalpine Böhler Welding Germany GmbH, 59067, Hamm, Germany
[h] RHP-Technology GmbH, 2444, Seibersdorf, Austria

ARTICLE INFO

Keywords:
Titanium alloys
Microstructure formation
Precipitation
Intermetallic phases
Atom probe tomography

ABSTRACT

Titanium alloys have been gaining importance in various industries due to their advantageous combination of strength, low density, excellent corrosion/oxidation resistance, and superior mechanical properties at elevated temperatures. Recently, eutectoid Ti–Cu alloys have been explored as promising candidates for advanced processes. This work investigates the effects of Fe and Al on a Ti-5.9Cu alloy using multi-scale characterization techniques. While Fe acts as a β-stabilizing element (despite being a sluggish eutectoid former), Al acts as an α-stabilizer. This work focuses on the effects of combined addition of these elements, studied in different heat treatment conditions. The results show that a fine, equiaxed microstructure is obtained in the binary Ti-5.9Cu alloy, whereas the addition of 2 wt% Fe, or 2 wt% Fe combined with 2 wt% Al to the Ti-5.9Cu alloy deteriorates the effect of grain refinement and coarse, columnar grains result and a small amount of β-phase is retained. Further, the microstructure resulting from the eutectoid decomposition is altered dramatically from a lamellar pearlitic in the binary alloy to a lath-like α-phase with diverse decomposition products in the ternary and quaternary alloys accompanied by increasing hardness values. Evaluation of the α misorientation suggests that a substantial amount of non-Burgers α is present in the Ti-Cu alloy in contrast to the results of the ternary and quaternary alloys. The observed Cu-rich intermetallic compound was identified as Ti_2Cu phase with off-stoichiometric composition. Results obtained explain how adding either Fe or Fe and Al leads to substantial hardening.

1. Introduction

Titanium alloys have been incorporated into modern aerospace structures since the early 1950s due to their high specific strength and stiffness, enabling lightweight design [1,2]. Thereby, efficiency is improved resulting in a reduction of the emission of environmentally detrimental pollutants [3] – a goal, which is outlined in today's strategic policies such as in Ref. [4].

Available commercial titanium alloys are classified based on their major constituent phases – a result of the allotropic modifications of titanium and the interplay of the respective phase stabilities with the alloying elements [1]. Most applications use wrought alloy grades relying on fine-grained microstructures resulting from recrystallization. Depending on the field of application, phase fractions and their morphologies are tailored to meet the specific criteria of usage. Modern advanced processes, such as additive manufacturing, require a more detailed understanding of the alloying effects on solidification and subsequent heat treatment to enable control of microstructure and properties.

Transition metals such as Cu, Ni, Fe or Co (to name a few) induce a eutectoid transformation, whereby the decomposition of the high temperature β-phase into α-phase and an intermetallic compound of varying

* Corresponding author. LKR Light Metals Technologies, AIT Austrian Institute of Technology, Lamprechtshausenerstr. 61, Ranshofen, 5282, Austria,
E-mail address: thomas.klein@ait.ac.at (T. Klein).

https://doi.org/10.1016/j.jmrt.2023.11.014
Received 14 September 2023; Received in revised form 30 October 2023; Accepted 1 November 2023
Available online 7 November 2023
2238-7854/© 2023 The Authors. Published by Elsevier B.V. This is an open access article under the CC BY-NC-ND license (http://creativecommons.org/licenses/by-nc-nd/4.0/).

stoichiometry occurs [5,6]. While a large body of literature deals with the effects of various α- and β-stabilizing elements, relatively few publications explore the effects of eutectoid forming elements or their interplay in complex ternary or quaternary alloys. Depending on the kinetics of decomposition, eutectoid forming elements are separated into *active* elements, where even on rapid cooling the transformation can hardly be suppressed, and *sluggish* elements, where long durations of annealing are required to induce the phase transformation. Although known for decades, no commercial alloys exploit the occurrence of eutectoid decompositions in titanium. Here, Fe is the exception as it can be used as a low-cost alternative for β-isomorph elements due to the extremely low eutectoid decomposition kinetics at low temperatures rendering this equilibrium transformation irrelevant. Recently, it has been demonstrated that in binary Ti-Cu alloys, the transformation results in a pearlitic microstructure [7–9]. Binary alloy variants, including alloys with e.g. Cu [7], Ni [10], Fe [11,12], or combinations thereof with ternary elements [13–15], have been shown to meet or even outperform mechanical properties of conventional Ti-6Al-4V. Other works report on the beneficial modification of the microstructure of Ti-6Al-4V through the addition of Cu [16–18], Ni [19], Fe [19–21], Co [22] or their combinations [23,24].

The present study was conducted as there is a clear deficit in the understanding of the vital role played by the addition of the *sluggish* transforming element Fe and the solid-solution strengthener Al on the eutectoid Ti-5.9Cu alloy. In this context, we therefore explore (i) how ternary and quaternary alloy modifications based on the Ti-5.9Cu system affect the solidification microstructure; (ii) how *sluggish* eutectoid forming elements (Fe) influence the eutectoid decomposition of an *active* eutectoid system (Ti-5.9Cu), and (iii) how the eutectoid transformation in the Ti-5.9Cu system and the mechanical properties are affected by the addition of an α-stabilizing element (Al), which is also a strong solid-solution strengthener. The in-depth studies to answer these three major research questions of the present work will provide fundamental knowledge to further design eutectoid titanium alloys. For this purpose, a multi-scale characterization campaign was launched encompassing scanning electron microscopy (SEM), including electron-backscatter diffraction (EBSD), X-ray diffraction (XRD), as well as high-resolution techniques including transmission electron microscopy (TEM) and atom probe tomography (APT). Gathered structural and chemical data is correlated to mechanical properties using microhardness measurements. The experimental results are corroborated using thermodynamic calculations. All data gained is merged to provide an in-depth understanding of the effects of Fe and Al on the pathways of phase transformation in the Ti-5.9Cu alloy providing a basis for the future exploitation of the eutectoid decomposition to design next generation titanium alloys.

2. Materials and methods

2.1. Alloy composition and processing

The investigated alloys were prepared as 20 g buttons from elemental materials Ti, Cu, Fe and Al pellets. Fabrication was conducted in an Edmund Bühler MAM-1 button arc-melter under Argon 5.0 protective atmosphere. Five consecutive remelting steps ensured chemical homogeneity as the tendency for segregation of the solutes is well documented [25–27]. Table 1 summarizes the nominal chemical compositions. The actual compositions are considered to closely match these as there is hardly any evaporation/oxidation under Argon conditions, and no spatter was observed. All chemical compositions referred to in this manuscript are given in weight percent unless specified otherwise. Subsequently, cylindrical specimens with 5 mm diameter and 10 mm length were fabricated and heat treated in a Bähr 805 A/D dilatometer, where they were short term aged at 600 °C for 15 min followed by rapid quenching with Helium.

Table 1
Nominal compositions of the alloys investigated in weight percent.

Alloy designation	Ti	Cu	Fe	Al
Ti-5.9Cu	bal.	5.9	–	–
Ti-5.9Cu-2Fe	bal.	5.9	2.0	–
Ti-5.9Cu-2Fe-2Al	bal.	5.9	2.0	2.0

2.2. Computational and experimental techniques

Phase fraction diagrams were calculated using Thermo-Calc 2021b with the TCTi3 thermodynamic database. Further, Scheil-Gulliver simulations without back-diffusion were used to calculate the freezing ranges of the alloys under investigation. The information obtained by these calculations was used to determine the growth restriction factor, Q [28] and the freezing range ΔT. The earlier can be calculated for multi component systems according to Eq. (1) [29]:

$$Q_{overall} \cong \sum_{i=1}^{n} C_{0,i} m_{L,i} (k_i - 1), \tag{1}$$

where $Q_{overall}$ includes the contributions of all solutes, $C_{0,i}$ refers to the nominal concentration of each solute, $m_{L,i}$ to the liquidus slope and k_i to each element's partitioning coefficient.

Microstructure characterization was conducted using a Mira 3 (Tescan) SEM in back-scattered electron (BSE) mode. The high-resolution BSE images were taken with a Gatan high signal-to-noise ratio (SNR) detector at 5 kV acceleration voltage. EBSD maps were collected at the center of the vertical cross-section of the buttons using a JOEL 7200F SEM at 20 kV. AZtecCrystal software was used for processing the EBSD data as well as the prior β-grain reconstruction and misorientation angle calculations.

Hardness values were determined using a DuraScan 70 G5 (Zwick-Roell) microhardness tester at 100 g load. Values reported correspond to mean values of at least five individual indents and the standard deviation is given alongside.

Local chemical compositions were analyzed using APT. For this purpose, a local electrode atom probe (LEAP 4000 X HR, Cameca) was used. After electrochemical polishing, the needle-shaped specimens were further sharpened using a Zeiss Auriga focused Ga-ion beam. The measurements were conducted in pulsed laser mode at 100 kHz with a laser energy of 50 pJ, a detection rate of 0.5 % and a sample temperature of 60 K. Data analysis was conducted using IVAS software version 3.6.14. The reconstructions were based on the voltage progression and the tips' geometries determined by SEM to guide the reconstruction.

XRD was performed with a X'pert powder diffractometer (Siemens) in Bragg-Brentano geometry with X'Celerator detectors. Cu-K_α-radiation was used, and the scans were conducted with steps of 0.02°. Phase analysis was performed with the X'pert HighScore software.

Samples for TEM analyses were prepared using an FEI Scios Dual Beam focused ion beam (FIB)-SEM. Bright field (BF) images and selected area diffraction pattern (SADP) were performed on a JEOL 2100F TEM at 200 kV.

3. Results and discussion

3.1. Prevalent phases with respect to alloy composition

Calculated phase fraction diagrams are shown in Fig. 1. In this figure, only β-phases and Cu-rich intermetallic compounds are shown for clarity as these are of highest interest when alloying the Ti-5.9Cu alloy with Fe and Al. Most importantly, the addition of Fe stabilizes the β-phase to room temperature, which is in agreement with its known β-stabilizing effect. Further, the addition of Al appears to stabilize a different variant of the Cu-rich intermetallic compound. While in the binary and the Fe-bearing alloy the formation of Ti_3Cu is predicted, in the quaternary

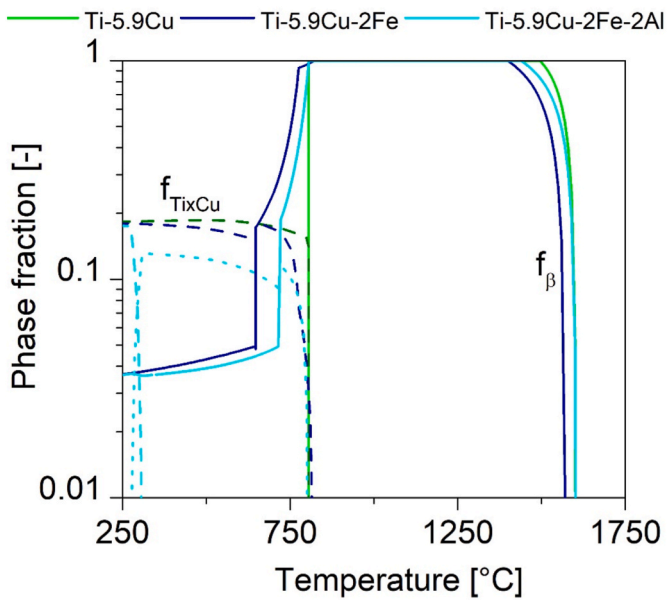

Fig. 1. Equibrium phase fraction diagram of the three investigated alloys showing only β-phases and Ti_xCu phases for clarity. Continuous lines correspond to the β-phase fraction, whereas dashed lines correspond to Ti_xCu phase fractions.

system Ti_2Cu forms, which transforms to Ti_3Cu on further cooling. The results of this calculation contradicts findings of Bhaskaran et al. [30] and more recently of Zhang et al. [7], who have shown experimentally that in binary Ti–Cu alloys Ti_2Cu is present, which is in agreement with the *ab initio* calculations available from Refs. [31,32] suggesting that the Ti_3Cu compound decomposes to Ti + Ti_2Cu under equilibrium conditions. For the moment we will refer to the prevalent intermetallic compound as Ti_xCu – its nature will be clarified in subsequently presented experimental analyses (see subsection 3.4).

3.2. Microstructure evolution and hardness

The EBSD inverse pole figure (IPF) maps after reconstruction of the β grains are shown in Fig. 2(a)–(c). Substantial differences in morphology and size of the grains, present in the three investigated alloys, are visible. In the case of the binary Ti-5.9Cu alloy (Fig. 2(a)) a fine-grained, equiaxed structure is visible, which is in agreement with recent findings [7]. Upon addition of Fe or Fe and Al, the size of the β grains is at least a factor of ten larger and an elongated/columnar grain structure is observed (Fig. 2(b) and (c)). Apparently, the grain refinement effect promoted by the addition of Cu – an effect of the large growth restriction factor as rationalized by the Interdependence Theory [7,28] – is poisoned by the addition of Fe. The local conditions at the interface of the moving solidification front and its interaction with diffusing solutes, in particular pertaining to their interplay with nucleation remains a difficult topic. Recent work by Tyagi et al. [33] illustrates the complexities of interacting phenomena upon solidification. As the transformation behavior of β-to α-phase is strongly affected (see later paragraphs in subsection 3.2) it remains unclear whether artifacts are introduced through the reconstruction procedure as has recently been analyzed by Saville and Clarke [34].

Recently, Nartu et al. [35] have used the growth restriction factor, Q, and the solidification range, ΔT, to predict the microstructure formed upon rapid solidification (additive manufacturing) of various titanium alloys suggesting that better agreement with experiments is obtained using the ΔT value. This train of thought was followed here, with the calculated results retrieved from Thermo-Calc according to Eq. (1) tabulated in Table 2. For comparison, both Q and ΔT were calculated.

Both, $Q_{overall}$ and ΔT, suggest that the ternary and quaternary alloys should solidify at least as fine and equiaxed as the binary alloy. It is, thus, unexpected that the ternary and quaternary alloys show a coarse microstructure. This means that other factors are affecting the grain refinement apart from the constitutional supercooling effect. These may include native nuclei of differing potency or density, or the effect of cycling through the eutectoid transformation [34]. While this observation is clearly backed by our results, its physical foundation needs further analysis and clarification beyond this work.

The microstructures of the three alloys are shown in Fig. 3 taken by

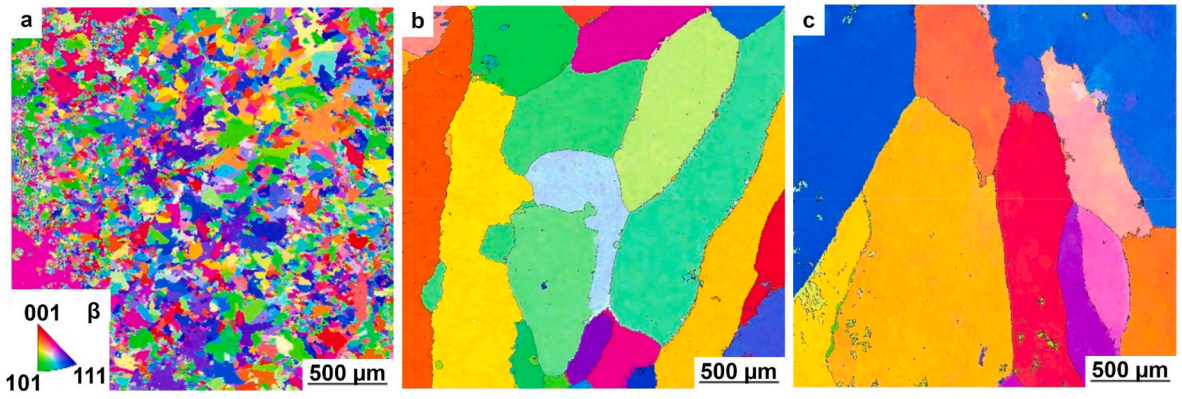

Fig. 2. Parent β grain reconstructed EBSD IPF maps of (a) Ti-5.9Cu; (b) Ti-5.9Cu-2Fe; and (c) Ti-5.9Cu-2Fe-2Al (all heat treated at 600 °C for 15 min). Ternary and quaternary alloying element additions clearly affect the prior β-grain structure.

Table 2
Summary of morphological description of primary β-phase from EBSD results, calculation results for the growth restriction factors and freezing ranges from Thermo-Calc.

Alloy	Observed grain morphology	$Q_{overall}$ [K]	ΔT [K]	Predicted grain morphology
Ti-5.9Cu	Fine, equiaxed	49	621.5	Equiaxed
Ti-5.9Cu-2Fe	Coarse, columnar	71	658.5	Equiaxed
Ti-5.9Cu-2Fe-2Al	Coarse, columnar	72	692.0	Equiaxed

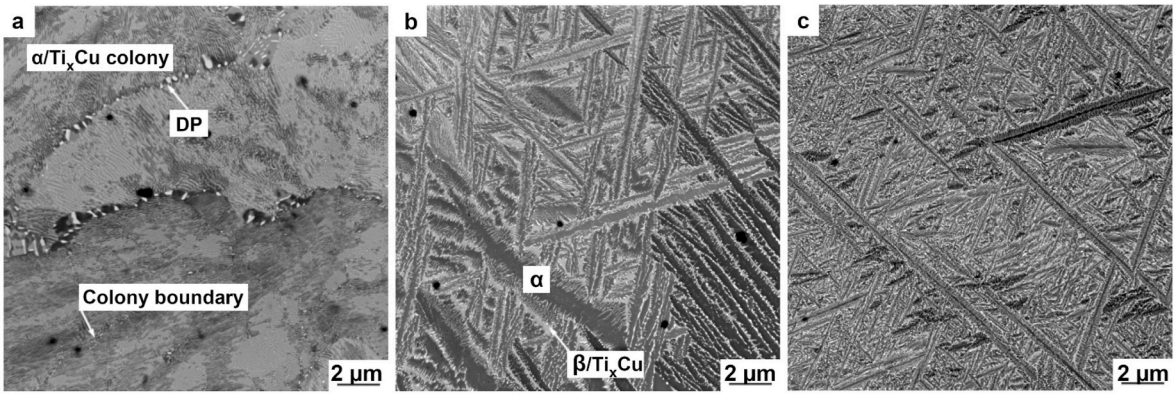

Fig. 3. SEM BSE micrographs of (a) Ti-5.9Cu; (b) Ti-5.9Cu-2Fe; and (c) Ti-5.9Cu-2Fe-2Al (all heat treated at 600 °C for 15 min). Ternary and quaternary alloying element additions clearly affect the mode of eutectoid decomposition.

SEM. The binary Ti-5.9Cu alloy shown in (a) comprises of a lamellar colony structure. These colonies are formed via coupled growth of the α-phase and Ti$_x$Cu at the expense of the decomposing parent β-phase as found in pearlite formation in steels [36,37]. Cardoso et al. [38] and Souza et al. [39] suggested that the precipitation of Cu-rich intermetallic phases cannot be suppressed in binary Ti–Cu alloys regardless of the cooling rate, which is in agreement with the *active* nature of the Ti–Cu eutectoid decomposition.

The colony boundaries visible in Fig. 3(a) are decorated by zones of discontinuous precipitation (DP), whereby the fine lamellar structure is consumed and coarser agglomerates with reduced interfacial energies/reduced interface areas remain [40]. The physical foundations of discontinuous reactions are established in Ref. [41]. The hardness values of the three alloys are summarized in Table 3. The hardness of the binary alloy is substantially below standard α + β alloys such as Ti-6Al-4V [42].

The addition of Fe changes the microstructure of the α-phase to lath-like features (Fig. 3(b)). A pronounced orientation contrast for the α-lamellae is visible. Bright phases with different contrast and a feathery microstructure are present along their boundaries. These are considered a mixed constituent of β-phases appearing bright due to large amounts of Fe, and Ti$_x$Cu also appearing bright due to high amounts of Cu. Such decomposition reactions have been reported by Bhaskaran et al. [30] and Cardoso et al. [38] occurring in Ti-Cu alloys with a martensitic microstructure, i.e., upon very high cooling rates. The observation of similar microstructural features in the present work in the alloys containing Fe after moderate cooling suggests that the diffusive decomposition is hindered by the presence of Fe. The likely cause is the substantial redistribution of Fe into the β-phase that is required for the α-phase to grow. Thus, diffusive growth of the α-phase is limited by the diffusivity of Fe in the β-phase (see subchapter 3.3 for detailed discussion of prevalent redistribution phenomena). Additionally, Fe also decreased the martensite start temperature by approximately 300 °C (addition of 2 wt%) according to Ref. [43]. The observed microstructural changes are associated with a substantial increase in hardness with respect to the binary alloy by $\Delta HV_{0.1} \approx 64$ (see Table 3).

Further, introducing Al to the ternary alloy system does not alter the morphological features of the microstructure in the alloy (Fig. 3(c)) in agreement with Oh et al. [44], which is backed by the fact that Al partitions toward the α-phase suggesting low effects on the interface mobility. However, a refinement of the α-laths is observed. As a result of this refinement, also the mixed β/Ti$_x$Cu constituent is significantly refined. Microstructural refinement and solid-solution strengthening by Al further increase the hardness by $\Delta HV_{0.1} \approx 61$, surpassing typical hardness values of Ti-6Al-4V [42].

Table 3
Summarized microhardness values of the investigated alloys.

Alloy	Ti-5.9Cu	Ti-5.9Cu-2Fe	Ti-5.9Cu-2Fe-2Al
Microhardness [HV0.1]	277 ± 17	341 ± 14	402 ± 14

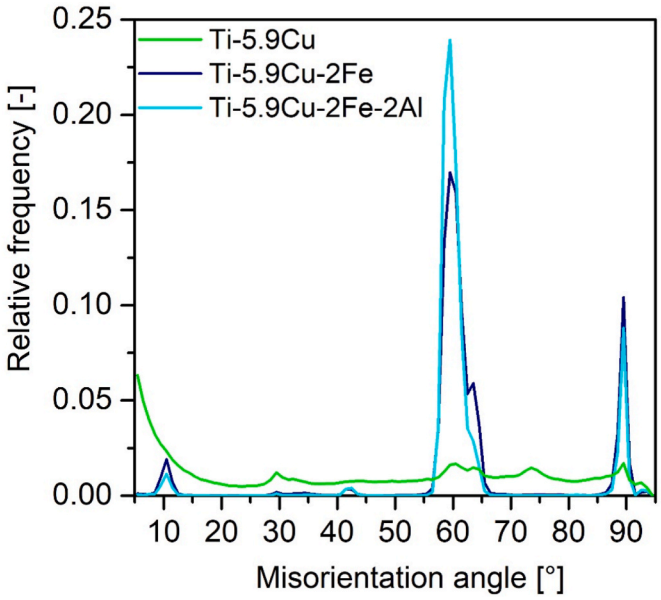

Fig. 4. Comparison of the misorientation angle distribution obtained from EBSD of the three investigated alloys evidencing distinct differences.

Fig. 4 shows the misorientation angle distribution evaluated from the EBSD map of all three alloys. The Ti-5.9Cu alloy shows a nearly random distribution, whereas Ti-5.9Cu-2Fe and Ti-5.9Cu-2Fe-2Al shows maxima at ~10°, ~55–65° and ~90°. These peaks result from intersecting α/α variants according to the Burgers orientation relationship. Equivalently, the absence of these peaks suggests that a substantial amount of non-Burgers α-phase is present in the microstructure (see Ref. [45] for further information on variant selection during phase transformations). These observations are in line with the previous work of Saville and Clarke [34], who have observed a substantial amount of non-Burgers α-phase in a binary pearlitic Ti-Cu alloy sample. It is worth noting that variant selection is a phenomenon commonly observed in Ti-6Al-4V or similar alloys processed, e.g., by different additive manufacturing processes [46]. Variant selection is, however, undesirable as it can promote strain localization, premature failure and can influence crack formation. Its suppression in the Ti-5.9Cu alloy is therefore considered beneficial.

3.3. Alloying element redistribution upon phase transformation

The phases present in the three considered alloy variants were

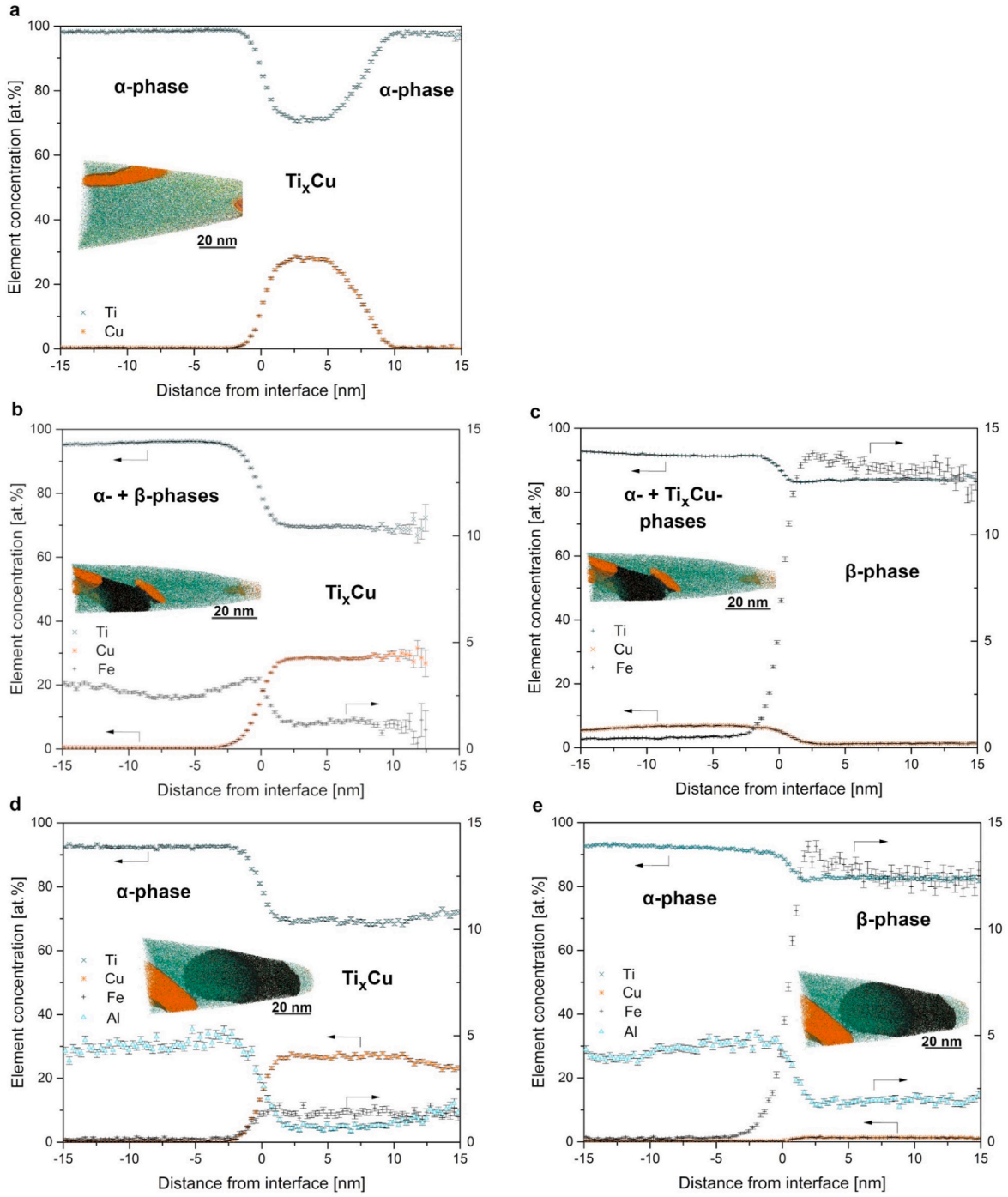

Fig. 5. Proximity histograms obtained using APT with the respective interfaces. (a) α/Ti$_x$Cu interface in Ti-5.9Cu; (b) α + β/Ti$_x$Cu interface in Ti-5.9Cu-2Fe; (c) α/Ti$_x$Cu interface in Ti-5.9Cu-2Fe-2Al; (d) α + Ti$_x$Cu/β interface in Ti-5.9Cu-2Fe; and (e) α/β interface in Ti-5.9Cu-2Fe-2Al.

studied by APT. Fig. 5 shows the proximity histograms calculated across the phase interfaces visible in the respective insets. The chemical compositions of the phases are given in Table 4 (for comparison the reader is referred to a recent work of Goettgens et al. [47], who have modified Ti-6Al-4V with Cu additions). The reconstructions of the binary alloy (Fig. 5(a)) prove enrichment of Cu in Ti$_x$Cu lamellae. The observed Cu concentration neither matches the stoichiometric compositions of Ti_3Cu nor Ti_2Cu phases. Therefore, the nature of the precipitate phase cannot be determined unambiguously by APT. The prevailing off-stoichiometric composition certainly suggests the presence of point defects in the ordered crystal lattice.

In the ternary Ti-5.9Cu-2Fe alloy two different phase boundaries were investigated (Fig. 5(b) and (c)). Similar Cu concentrations in the Cu-rich intermetallic are observed in comparison to the binary alloy. At both interphase boundaries, the Fe distribution is particularly interesting. Its enrichment in the β-phase is clearly visible, while the α-phase is depleted. This observation is clearly in line with the β-stabilizing effect of Fe. Also, Ti$_x$Cu phase seems to be depleted in Fe (less pronounced). At both identified interphase boundaries, the Fe content is higher in the β-side with a 'pile up' near the interface. This is typical for a moving interface and a slow diffusing element [48]. As no interface could be delineated that would solely allow discriminating the α-phase, the mass balance was used to estimate the chemical composition given in Table 4 according to Eq. (2):

Table 4
Chemical compositions of the constituent phases determined from the APT proximity histograms given in atomic percent.

Alloy	Phase	Ti	Cu	Fe	Al	Others
Ti-5.9Cu	α	98.62	0.35	0.11	0.05	0.87
	Ti_xCu	71.21	28.17	0.09	0.04	0.49
Ti-5.9Cu-2Fe	α[a]	99.56	0.00	0.02	0.03	0.39
	β	83.46	1.30	12.91	0.83	1.50
	Ti_xCu	69.39	28.40	1.10	0.10	1.01
Ti-5.9Cu-2Fe-2Al	α	92.84	0.35	0.15	4.48	2.18
	β	82.83	1.40	12.57	1.97	1.23
	Ti_xCu	69.21	27.13	1.39	0.73	1.54

[a] Calculated from mass balance given in Eq. (2).

$$c^j_{overall} = \sum_{i=1}^{3} f_i c^j_i \quad (2)$$

where $c^j_{overall}$ refers to the overall concentration of element j, f_i is the phase fraction of each phase (here taken from thermodynamic simulation), and c^j_i is the concentration of element j in phase i.

The proximity histograms of the Ti-5.9Cu-2Fe-2Al alloy show similar behavior with regard to Cu enrichment in Ti_xCu and Fe enrichment in the β-phase (interfacial 'pile-up' again visible). At these interfaces the redistribution behavior of Al can be studied. In Fig. 5(d) substantial enrichment of Al in the α-phase is visible, which aligns well with known α-stabilizing effect, and concomitantly its depletion in both Ti_xCu and β-phase is observed. A small 'pile-up' of Al at the α-phase side is observed – a result of its limited atomic mobility resulting in incomplete redistribution during thermal exposure and the accompanying phase transformation.

3.4. Structural characterization of the Cu-rich intermetallic compound

XRD was used to determine the crystallography of the present major phases (Fig. 6). It is noted that the intensity may be affected by textures present in the button samples resulting from the solidification conditions, thus, prohibiting quantitative phase analysis. However, the dominance of the α-phase in all three investigated alloys is clearly visible and the introduction of the β-phase through the addition of Fe can be observed, which agrees well with the thermodynamic predictions and APT results. The weak peaks linked to the Cu-rich intermetallic

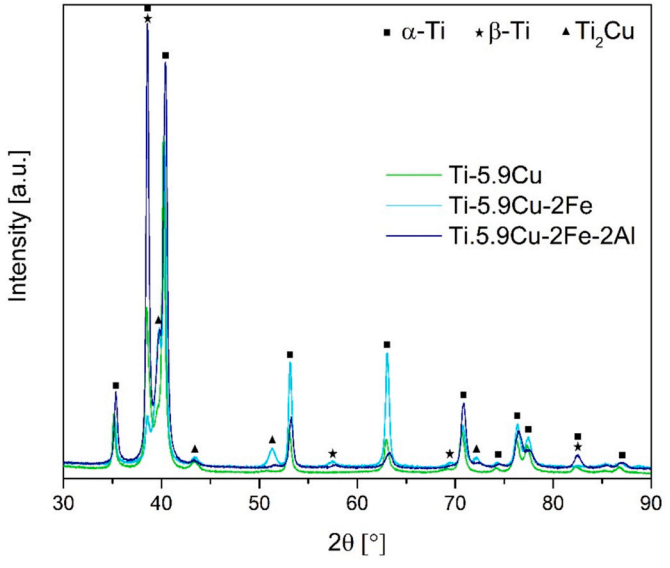

Fig. 6. XRD diffractograms of the investigated alloys with the major phases indicated.

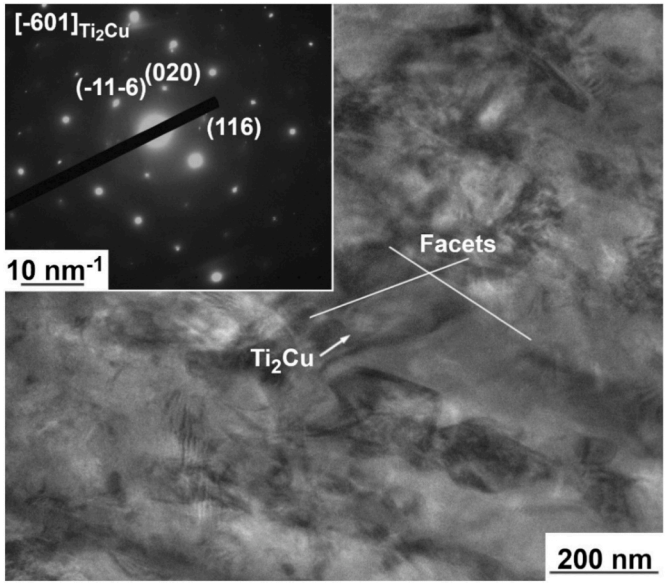

Fig. 7. TEM BF image of a Ti_2Cu particle with the SADP as inset evidencing its crystallographic nature.

compound can be entirely indexed with the Ti_2Cu structure in all alloys and not the Ti_3Cu phase. For the binary alloy this observation is in agreement with recent works by Zhang et al. [7] and Saville et al. [49].

To further analyze the Ti_2Cu particles, TEM was used for the Ti-5.9Cu-2Fe-2Al alloy. A bright field image is shown in Fig. 7(a) together with the indexed selected area diffraction pattern in Fig. 7(b). The nm-scaled particle (~100–200 nm) marked in Fig. 7 shows faceted morphology and can be unambiguously indexed as the Ti_2Cu crystallographic structure (space group: I4/mmm; a = b = 0.297 nm; c = 1.0899 nm [50]) shown as inset in Fig. 7. The observed structure is similar to the detailed results of the study of Ng et al. [51], who investigated alloy variants of Ti-10V alloys modified with either Ni or Cu.

3.5. Technological implications

3.5.1. Solidification microstructure and hardness

Cu-modified titanium alloys are considered as prime candidates for manufacturing processes such as casting or additive manufacturing that do not employ thermo-mechanical processing. Beneficial effects on the grain structure in terms of a fine and equiaxed structure essentially free of texture were reported [7]. The present study reveals that appropriate solidification conditions are achieved using button arc-melting in the binary Ti-Cu alloy system. However, the addition of Fe or mixed additions of Fe and Al alter the solidification conditions in a way that very fine grains were not observed, i.e., reversing the refinement effect induced by Cu. Different hypotheses from the literature remain, however, unable to unambiguously explain this behavior.

Alloying with Fe or Fe and Al results in substantial hardening. Therefore, it is concluded that both elements Fe and Al are capable of improving the mechanical performance of Ti-Cu alloys. Future work will therefore focus on (i) identification of the underlying mechanisms of grain refinement poisoning induced by Fe or Fe and Al, (ii) identification of suitable alloying element additions that equally harden the alloy without deteriorating the fine-grained β grain structure.

3.5.2. Eutectoid decomposition and Ti_2Cu precipitation

The eutectoid phase transformation during the present processing conditions is clearly altered by the introduction of ternary and quaternary alloying elements (see Fig. 3). On the one hand, this is clearly visible in terms of morphology of the α- and the Ti_2Cu-phases (identified by XRD and TEM), on the other hand, it is underpinned by different

α-phase variant selection. These changes can be employed to design specific heat treatments in the future allowing for balanced mechanical properties.

The chemical compositions of the individual phases reveals low solubilites of the Ti_2Cu-phase for both Fe and Al. Thus, substantial solute redistribution is required during its nucleation and growth. The temporal dependence of these processes induces the observed morphological changes in the ternary and quaternary alloy systems and can be used to specifically design the precipitate size distribution upon heat treatment.

4. Conclusions

Titanium alloys exploiting the beneficial effects of Cu on the primary grain formation and its solid-state eutectoid reaction have been suggested as promising candidate materials to be used in future advanced processing. Further alloying refinement is suggested in the present work to modify the microstructure evolution. This work reports on the effects of Fe and Al on the eutectoid Ti-5.9(wt.%)Cu alloy. To understand the resultant microstructural changes, a multi-scale characterization approach was chosen. From the performed analyses the following major conclusions can be drawn:

* The addition of Fe stabilizes the β-phase to ambient temperatures. The cooperative growth occurring during the eutectoid decomposition of the binary alloy is altered to a consecutive reaction with lath-like α-features and small Cu-rich precipitates. This variation of solid-state reaction affected the fine-scaled microstructural features and, thereby, led to a drastic increase in the hardness.
* The addition of Al has little effect on the phases in comparison to the ternary alloy variant (Ti-5.9Cu–2Fe) except for refinement of the α lamellae. Also, Al substantially increases the hardness of the material, which is argued to be a result of solid-solution strengthening.
* The beneficial effects of Cu on the primary β grain size and morphology seem to be poisoned through the additions of Fe or Fe and Al. While the binary alloy is dominated by fine, equiaxed grains, the ternary and quaternary alloys are composed of large and columnar grains.
* The alloying element additions strongly influence the α-phase variant selection. While the dominant variants in the ternary and quaternary alloy reflect the dominant transformation mode, a rather diffuse distribution of variants is observed in the binary alloy suggesting that the Burgers orientation relationship is not prevalent during cooperative, pearlite-like growth.
* The Cu-rich intermetallic phase was identified as the Ti_2Cu phase crystallographically. Its chemical composition is, however, off-stoichiometric.

In this work, it is shown that the addition of β-stabilizing elements to the eutectoid Ti–Cu system provides a suitable means to modify and control the solid-state transformation pathway. The presented research provides the basis for future exploitation of tailored titanium alloy compositions based on the Ti–Cu system. Future research directions should focus on the alloy design and accompanying heat treatment procedures resulting in optimum microstructures and properties following solid-state transformations, while maintaining a fine primary β grain structure, free of solidification texture.

Funding

This research has been funded by the Austrian Federal Ministry for Climate Action, Environment, Energy, Mobility, Innovation and Technology (BMK) within the aeronautics funding program "Take Off", project "highTi – Novel high-strength titanium alloys for aeronautic applications" (grant agreement no. 886889) administered by FFG. D.Z. would like to thank the support of ARC-DECRA grant (No. DE210101503). D.Q. and M.E. appreciate the financial support of ARC Discovery grant (No. DP220101501).

Declaration of competing interest

The authors declare that they have no known conflicts of interest that could have appeared to influence the work reported in this paper.

Acknowledgements

Technical assistance by I. Baumgartner, R. Hellstern, A. Arnoldt (all LKR) and M. Weinhard (KNMFi) is greatly appreciated. The authors acknowledge the facilities, and the scientific and technical assistance of the RMIT Microscopy & Microanalysis Facility (RMMF), a linked laboratory of Microscopy Australia, enabled by NCRIS and at the Karlsruhe Nano Micro Facility (KNMFi, www.knmf.kit.edu), with proposal no 2022–028031387.

References

[1] Froes FH. Titanium: physical metallurgy, processing and applications. Materials Park, OH: ASM International; 2015.
[2] Jaffee RI. The physical metallurgy of titanium alloys. Prog Met Phys 1958;7:65–163. https://doi.org/10.1016/0502-8205(58)90004-2.
[3] Williams JC, Boyer RR. Opportunities and issues in the application of titanium alloys for aerospace components. Metals 2020;10. https://doi.org/10.3390/met10060705.
[4] Roadmap to decarbonising European aviation, https://www.transportenvironment.org/discover/roadmap-decarbonising-european-%0Aaviation/(accessed July 18, 2023).
[5] Lee HJ, Aaronson HI. Eutectoid decomposition mechanisms in hypoeutectoid Ti-X alloys. J Mater Sci 1988;23:150–60. https://doi.org/10.1007/BF01174047.
[6] Bhaskaran TA, Krishnan RV, Ranganathan S. On the decomposition of β phase in some rapidly quenched titanium-eutectoid alloys. Metall Mater Trans A 1995;26:1367–77. https://doi.org/10.1007/BF02647587.
[7] Zhang D, Qiu D, Gibson MA, Zheng Y, Fraser HL, StJohn DH, et al. Additive manufacturing of ultrafine-grained high-strength titanium alloys. Nature 2019;576:91–5. https://doi.org/10.1038/s41586-019-1783-1.
[8] Donthula H, Vishwanadh B, Alam T, Borkar T, Contieri RJ, Caram R, et al. Morphological evolution of transformation products and eutectoid transformation (s) in a hyper-eutectoid Ti-12 at% Cu alloy. Acta Mater 2019;168:63–75. https://doi.org/10.1016/j.actamat.2019.01.044.
[9] Devaraj A, Nag S, Muddle BC, Banerjee R. Competing martensitic, bainitic, and pearlitic transformations in a hypoeutectoid Ti-5Cu alloy. Metall Mater Trans A Phys Metall Mater Sci 2011;42:1139–43. https://doi.org/10.1007/s11661-011-0656-5.
[10] Narayana PL, Kim JH, Lee S, Won JW, Park CH, Yeom JT, et al. Novel eutectoid Ti-5Ni alloy fabricated via direct energy deposition. Scripta Mater 2021;200:113918. https://doi.org/10.1016/j.scriptamat.2021.113918.
[11] Klein T, Paul MJ, Simson C, Niedermayer J, Gludovatz B. Phase decomposition upon heat-treatment of a eutectoid Ti-Fe alloy processed by dual-wire-arc additive manufacturing. Mater Lett 2022;319:132305. https://doi.org/10.1016/j.matlet.2022.132305.
[12] Song T, Chen Z, Cui X, Lu S, Chen H, Wang H, et al. Strong and ductile titanium–oxygen–iron alloys by additive manufacturing. Nature 2023;618:63–8. https://doi.org/10.1038/s41586-023-05952-6.
[13] Mellor RFL, Vacek P, Jones NG, Midgley PA, Stone HJ. Precipitate nanostructuring that enhances lattice compatibility in a Ti-Fe-Al alloy. Scripta Mater 2023;232:115476. https://doi.org/10.1016/j.scriptamat.2023.115476.
[14] Pfaffinger V, Staufer E, Edtmaier C, Arnoldt A, Schmitz-Niederau M, Horky J, et al. Insights into phase evolution and mechanical behavior of the eutectoid Ti–6.4(wt%)Ni alloy modified with Fe and Cr. Adv Eng Mater 2023;25:2300177. https://doi.org/10.1002/adem.202300177.
[15] Zhao D, Chen Y, Jiang C, Li Y, Zhao Q, Xu Y, et al. Morphological evolution of Ti2Cu in Ti-13Cu-Al alloy after cooling from semi-solid state. J Alloys Compd 2020;848. https://doi.org/10.1016/j.jallcom.2020.156639.
[16] Li X, Yao Z, Tao X, Yao M, Zhang S. Developing Cu modified Ti6Al4V alloys with a combination of high strength and ductility by electron beam freeform fabrication. Vacuum 2021;194:110638. https://doi.org/10.1016/j.vacuum.2021.110638.
[17] Zykova A, Nikolaeva A. Effect of copper content on grain structure evolution in additively effect of copper content on grain structure evolution in additively manufactured Ti-6Al-4V alloy. Phys Mesomech 2023;23:107–25. https://doi.org/10.1134/S1029959923020017.
[18] Vilardell AM, Yadroitsev I, Yadroitsava I, Albu M, Takata N, Kobashi M, et al. Manufacturing and characterization of in-situ alloyed Ti6Al4V(ELI)-3 at.% Cu by laser powder bed fusion. Addit Manuf 2020;36. https://doi.org/10.1016/j.addma.2020.101436.
[19] Welk BA, Taylor N, Kloenne Z, Chaput KJ, Fox S, Fraser HL. Use of alloying to effect an equiaxed microstructure in additive manufacturing and subsequent heat

treatment of high-strength titanium alloys. Metall Mater Trans A 2021;52:5367–80. https://doi.org/10.1007/s11661-021-06475-3.
[20] Simonelli M, McCartney DG, Barriobero-Vila P, Aboulkhair NT, Tse YY, Clare A, et al. The influence of iron in minimizing the microstructural anisotropy of Ti-6Al-4V produced by laser powder-bed fusion. Metall Mater Trans A 2020;51:2444–59. https://doi.org/10.1007/s11661-020-05692-6.
[21] Chen M, Van Petegem S, Zou Z, Simonelli M, Tse YY, Chang CST, et al. Microstructural engineering of a dual-phase Ti-Al-V-Fe alloy via in situ alloying during laser powder bed fusion. Addit Manuf 2022;59:103173. https://doi.org/10.1016/j.addma.2022.103173.
[22] Choi G, Choi WS, Han J, Choi PP. Additive manufacturing of titanium-base alloys with equiaxed microstructures using powder blends. Addit Manuf 2020;36:101467. https://doi.org/10.1016/j.addma.2020.101467.
[23] Zhang T, Zhu J, Yang T, Luan J, Kong H, Liu W. A new α + β Ti-alloy with refined microstructures and enhanced mechanical properties in the as-cast state. Scripta Mater 2022;207:114260. https://doi.org/10.1016/j.scriptamat.2021.114260.
[24] Su J, Jiang F, Tan C, Weng F, Lan F, Hao M, et al. Additive manufacturing of fine-grained high-strength titanium alloy via multi-eutectoid elements alloying. Compos Part B 2023;249:110399. https://doi.org/10.1016/j.compositesb.2022.110399.
[25] Gao L, Huang H guang, Kratzsch C, Zhang H ming, Chattopadhyay K, Jiang Y hua, et al. Numerical study of aluminum segregation during electron beam cold hearth melting for large-scale Ti-6 wt%Al-4 wt%V alloy slab ingots. Int J Heat Mass Transf 2020;147:118976. https://doi.org/10.1016/j.ijheatmasstransfer.2019.118976.
[26] Zeng WD, Zhou YG. Effect of beta flecks on mechanical properties of Ti-10V-2Fe-3Al alloy. Mater Sci Eng A 1999;260:203–11. https://doi.org/10.1016/s0921-5093(98)00954-x.
[27] Ng CH, Bermingham MJ, Yuan L, Dargusch MS. Towards β-fleck defect free additively manufactured titanium alloys by promoting the columnar to equiaxed transition and grain refinement. Acta Mater 2022;224:117511. https://doi.org/10.1016/j.actamat.2021.117511.
[28] StJohn DH, Qian M, Easton MA, Cao P. The Interdependence Theory: the relationship between grain formation and nucleant selection. Acta Mater 2011;59:4907–21. https://doi.org/10.1016/j.actamat.2011.04.035.
[29] Mitrašinović AM, Robles Hernández FC. Determination of the growth restriction factor and grain size for aluminum alloys by a quasi-binary equivalent method. Mater Sci Eng A 2012;540:63–9. https://doi.org/10.1016/j.msea.2012.01.072.
[30] Bhaskaran TA, Krishnan RV, Srinivasa Raghavan K. The decomposition of hexagonal martensite in a titanium-copper alloy. Scripta Metall 1985;19:319–22. https://doi.org/10.1016/0036-9748(85)90322-9.
[31] Persson K. Materials data on Ti2CU (SG:139) by materials project. Mater Proj 2016. https://doi.org/10.17188/1287957.
[32] Persson K. Materials data on Ti3Cu (SG:221) by materials project. Mater Proj 2014. https://doi.org/10.17188/1187766.
[33] Tyagi S, Monteux C, Deville S. Multiple objects interacting with a solidification front. Sci Rep 2021;11:1–14. https://doi.org/10.1038/s41598-021-82713-3.
[34] Saville AI, Clarke AJ. Reconstructing parent microstructures in martensitic and pearlitic Ti-Cu. Mater Char 2023;196:112569. https://doi.org/10.1016/j.matchar.2022.112569.
[35] Nartu MSKKY, Welk BA, Mantri SA, Taylor NL, Viswanathan GB, Dahotre NB, et al. Underlying factors determining grain morphologies in high-strength titanium alloys processed by additive manufacturing. Nat Commun 2023;14:3288. https://doi.org/10.1038/s41467-023-38885-9.
[36] Zhang MX, Kelly PM. The morphology and formation mechanism of pearlite in steels. Mater Char 2009;60:545–54. https://doi.org/10.1016/j.matchar.2009.01.001.
[37] Bhadeshia HKDH. Bainite in steels. third ed. Boca Raton, Florida: CRC Press; 2015.
[38] Cardoso FF, Cremasco A, Contieri RJ, Lopes ESN, Afonso CRM, Caram R. Hexagonal martensite decomposition and phase precipitation in Ti-Cu alloys. Mater Des 2011;32:4608–13. https://doi.org/10.1016/j.matdes.2011.03.040.
[39] Souza SA, Afonso CRM, Ferrandini PL, Coelho AA, Caram R. Effect of cooling rate on Ti-Cu eutectoid alloy microstructure. Mater Sci Eng C 2009;29:1023–8. https://doi.org/10.1016/j.msec.2008.09.007.
[40] Guyon J, Hazotte A, Wagner F, Bouzy E. Recrystallization of coherent nanolamellar structures in Ti48Al2Cr2Nb intermetallic alloy. Acta Mater 2016;103:672–80. https://doi.org/10.1016/j.actamat.2015.10.049.
[41] Williams DG, Butler EP. Grain boundary discontinuous precipitation reactions. Int Met Rev 2013;26:153–83. https://doi.org/10.1179/imtr.1981.26.1.153.
[42] Keist JS, Palmer TA. Development of strength-hardness relationships in additively manufactured titanium alloys. Mater Sci Eng A 2017;693:214–24. https://doi.org/10.1016/j.msea.2017.03.102.
[43] Neelakantan S, Rivera-Díaz-del-Castillo PEJ, van der Zwaag S. Prediction of the martensite start temperature for β titanium alloys as a function of composition. Scripta Mater 2009;60:611–4. https://doi.org/10.1016/j.scriptamat.2008.12.034.
[44] Oh ST, Woo K Do, Kim JH, Kwak SM. The effect of al and v on microstructure and transformation of β phase during solution treatments of cast ti-6al-4v alloy. J Korean Inst Met Mater 2017;55:150–5. https://doi.org/10.3365/KJMM.2017.55.3.150.
[45] Furuhara T, Maki T. Variant selection in heterogeneous nucleation on defects in diffusional phase transformation and precipitation. Mater Sci Eng A 2001;312:145–54. https://doi.org/10.1016/S0921-5093(00)01904-3.
[46] Farabi E, Klein T, Schnall M, Primig S. Effects of high deposition rate during cold metal transfer additive manufacturing on microstructure and properties of Ti-6Al-4V. Addit Manuf 2023;71:103592. https://doi.org/10.1016/j.addma.2023.103592.
[47] Goettgens VS, Kaserer L, Braun J, Busch R, Berthold L, Patzig C, et al. Microstructural evolution and mechanical properties of Ti-6Al-4V in situ alloyed with 3.5 wt.% Cu by laser powder bed fusion. Materialia 2023;32:101928. https://doi.org/10.1016/j.mtla.2023.101928.
[48] Felfer P, Scherrer B, Demeulemeester J, Vandervorst W, Cairney JM. Mapping interfacial excess in atom probe data. Ultramicroscopy 2015;159:438–44. https://doi.org/10.1016/j.ultramic.2015.06.002.
[49] Saville AI, Hesmondhalgh OW, Compton NA, Thompson GA, Sanders M, Klemm-Toole J, et al. Fine-grained Ti-Cu microstructures by solid state thermal cycling. Addit Manuf 2023:129074. https://doi.org/10.1016/j.addma.2023.103747.
[50] Schubert R. Über die Verbreitung des Zr2Cu-Typs und Cr2Al-Typs. Zeitschrift Fuer Met 1964;55:798–804.
[51] Ng HP, Douguet E, Bettles CJ, Muddle BC. Age-hardening behaviour of two metastable beta-titanium alloys. Mater Sci Eng A 2010;527:7017–26. https://doi.org/10.1016/j.msea.2010.07.055.